

Original Article

# Dental Diseases Segmentation

S. Hemalatha<sup>1</sup>, R. Karthika Devi<sup>2</sup>

<sup>1</sup>Sethu Institute of Technology, Virudhunagar

<sup>2</sup>Department of Electronics and Communication, Anna University, Chennai, India

Received : 11 December 2021

Revised : 12 January 2022

Accepted : 23 February 2022

Published : 28 February 2022

**Abstract** - In recent times, dental care detection has been much needed for society. The dental care prediction is performed with innovative automation using Deep learning (DL) techniques. The earlier prediction is the main problem in the dental field that also leads to heavy illness of health. To overcome these issues, segmentation is to be performed effectively. Therefore, this paper presents the DL-based Butterfly-net model to perform an efficient dental care prediction. This butterfly Net algorithm is based on Deep Convolutional Neural Network (DCNN) that is used to classify dental images. This butterfly net algorithm can be evaluated as a dental degree of membership. The proposed work is compared with the previous work where the Butterfly-net has the highest classification accuracy among all.

**Keywords** - Dental care, DCNN, Butterfly net, Classification, Prediction.

## 1. Introduction

In the present, there is a huge change in the existence of individuals and their well-being habits. The principal issue among kids is their tooth issues. Different tooth issues are emerging among youngsters in light of their unfortunate dietary habits. It is considered a primary issue since this defaulting construction of teeth or hole can create many issues in the later existence of these youngsters. The most well-known issues among these kids are a projection of long-lasting teeth before teeth falling either frontward or in reverse and another pit issue that emerges from eating a lot of sweet things.

It is considered one of the fundamental issues of kids. Further, in this paper, the profundity between the deciduous teeth and long-lasting teeth is determined, and it is likewise analysed where there is a hole present in the teeth. Dental caries is one of the most well-known preventable sicknesses, which is perceived as the essential driver of oral pain and tooth loss[3]. It is a significant general well-being oral infection that frustrates the accomplishment and upkeep of oral well-being in all age gatherings.

An efficient classification is performed using a DL technique [4] to overcome these issues. In particular, DCNN has ended up being an integral asset in image acknowledgement and representation. DL has likewise arisen to be effectively applied in taking care of physics issues, showing the capability of turning into an instrument of incredible use for computational mathematics and physics, too [5]. In this work, Butterfly-nets-based CNN is presented, which comprises convolutional and transpose convolutional layers with sparse cross-channel connections, plus a locally connected switch layer in between. This proposed Butterflynets is used to provide an approximate Fourier kernel. This process can be used to predict dental health effectively.

The rest of the work is sorted as section 2 provides literature works on dental health care. Section 3 discussed a proposed methodology and section 4 described the result and discussion. The conclusion is summarised in section 5 and followed by a reference.

## 2. Literature Survey

This section carried previous literature-related work based on the dental health abnormalities below.

AbdolvahabEhsani Rad et al. [7] presented a review for teeth segmentation utilising two unique thresholding methods. The exhibitions of these methods are contrasted and one another. The outcomes showed a perceptible distinction in segmentation quality between the two techniques introduced in this paper.

Mahmoud Al-Ayyoub et al. [8] discussed an observing ROI for both gap valley and tooth isolation utilising binary edge intensity. The calculation utilises a district-developing methodology followed by a Canny edge identifier. It naturally finds the ROI both for gap valley and tooth isolation in dental radiograph images without revolution.

Weng-Kong Tam et al. [9] developed wavelet transform (WT) to section dental X-beam images. Wavelet transform is little waves situated at various times that dissect as indicated by the scale. The consequence of segmentation is teeth, including denoting every pixel. For example, edges recognition from image portioned.

Sudhakar T et al. [10] presented two image-handling techniques for dental anomaly identification. This technique is used to identify dental caries utilising hybridised negative transformation. The second part is presented a statistical texture investigation for the dental images containing pimples alongside dental caries. The



texture examination is utilised when the items are divided in view of texture content rather than powers.

Rad AE et al. [11] investigated the consequences of extraction of the tooth and dental work shape. These are utilised in matching two radiographs and coordinating to recognise people. It presented a matching of two radiographs in light of histogram properties, tooth area, and dental work.

BalaSubr:amanyam et al. [12] introduced a technique to naturally measure the dental plaque in dental images utilising mean shift. This approach was applied to a clinical information base comprising 30 articles. The outcomes show that the proposed strategy gave a precise quantitative estimation of dental plaque contrasted and that of conventional manual estimation files of dental plaque. LaiY.H et al. [13] introduced an approach for automatically evaluating dental plaque because of adjusted kernelised fuzzy c-means. This approach was applied to a clinical information base consisting of 30 objects. The outcomes show that this technique gives an accurate quantitative estimation of dental plaque compared with manual estimation indices of the dental plaque.

AbdolvahabEhsani Rad et al. [14] introduced a technique to extract the rebuilding part from the dental X-ray image by combining the Fuzzy clustering with the iterative level set active contour. Right off the bat, we utilise the Preprocessing utilising median filtering to eliminate the clamour present in the X-ray image, so it tends to be utilised for additional processing. Secondly, Fuzzy clustering is used for image segmentation to recognise various clusters. Finally, a Level set active contour strategy is applied to extract the rebuilding region from the teeth. The accuracy of this technique is obtained efficiently.

AnifHanifaSetianingrum et al. [15] described image segmentation utilising the Otsu technique on dental X-rays. It can help distinguish tooth decay by setting the Otsu result's edge worth. There was a decrease in the limit of an incentive for the images of solid dental compared to the images of sick teeth under the two conditions of applying image enhancement and without image enhancement.

Hao Wang et al. [16] presented an efficient structure that achieves tooth segmentation in light of the segmentation field. Especially the candidate cutting limits can be detected from the concave areas with huge varieties of field information. The result shows that the normal Peak Signal-to-Noise Ratio (PSNR) has been acquired at 19.98 and 20 by applying K-means clustering and limit technique, respectively, alongside a satisfactory visual understanding of the three-layered structure of dental caries.

### 3. Proposed System

The proposed block diagram is shown in figure 1, which comprises an input dataset of dental images, pre-processing, and modified Butterfly-net for segmentation and result.

The dataset is collected from the dental clinic dataset website of Dental Utilization By Provider - CY 2018. It included service counts and beneficiaries for dental visits of a year, preventive services, treatment, and exams related to the dental by providers.

#### 3.1. Pre-Processing

Pre-processing is the essential step of image processing. It can handle the pre-processing image and convert it into RGB to greyscale images. This step processed a conversion, transformation and re-sizing of the input image into processing size.

Next, the data set is classified for testing and training. 70 percent of the data is used for the training model, and 30 percent of the data is used for the testing model.

#### 3.2. Segmentation

The segmented data features are extracted to identify the dental abnormalities data in the segmentation process. It is processed by using a Modified Butterfly-Net technique. The Modified Butterfly Net is used for segmentation based on the DCNN strategy. It is a minimum complexity architecture of CNN and sparse cross-channel connections in the network.

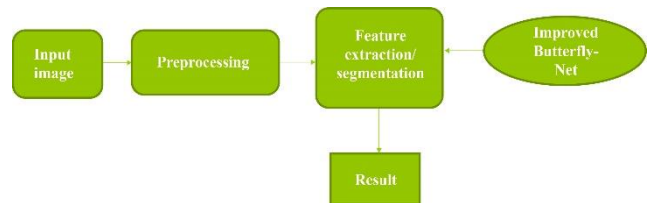


Fig. 1 Proposed system

The training data is processed by this modified Butterfly-net, which has a Fourier representation data with an error that decays exponentially as the depth increases.

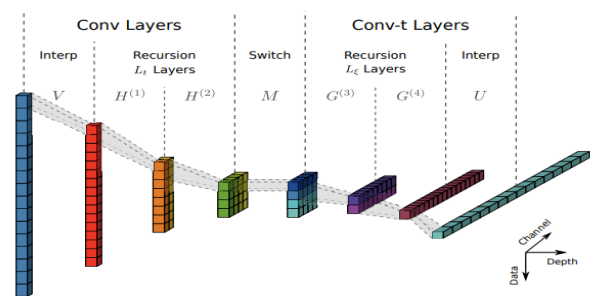


Fig. 2 Modified butterfly net architecture

This butterfly combines a fully connected CNN with network complexity depending on the effective bandwidth frequency. The Fourier kernels approximation and energy functionals of Poisson's equations are evaluated. The architecture of Butterfly-net is discussed below.

#### 3.3. Butterfly-net Architecture

For each layer, the CNN architecture is trailed by specifying the pre-characterised Butterfly introduction and an explanation connected with the Fourier transform.

Let  $x(t)$  be the information considered a signal in time. For the most part, time-frequency investigation

decomposes the signal into various modes according to frequency range, e.g., high-, medium-, and low-frequency modes. In particular, once the signal is decomposed into various modes, they are examined independently and won't be mixed again. It corresponds to the non-mixing channel thought in Butterfly-net, and the non-mixing channel explicitly corresponds with frequency modes. The information vector is of length N, and the result is a feature vector of length K. Give L indicates the number of significant layers that access the Butterfly net, and r signifies the size of mixing channels.

To initialise the butterfly net, then the switch Layer (L) is expressed as

$$L = L_t + L_\xi \quad (1)$$

Where  $L_t$  indicates some layers before the switch layer and  $L_\xi$  denotes the number of layers after the switch layer.

A general tensor notation  $\lambda^{(l)}(i, j, k)$  is presented in this method that corresponds to Butterfly coefficients is given as

$$\lambda^{(l)}(i, j, k) = \lambda_k^{A_i^l B_j^{L-l}} \quad (2)$$

where k represents the mixing channel, the index i represents the non-mixing channel and j represents the data dimension. The index range of l, i, and j is identified.

The following operations are performed by a butterfly-net method:

i) Interpolation ( $l = 0$ ), the weight tensor is expressed as

$$W_{k,q,1}^{(0)} \stackrel{\diamond}{=} e^{-2\pi i \xi_0 (t_q - t_k)} \mathcal{L}_k(t_q), \quad 1 \leq k \leq r \text{ and } 1 \leq q \leq m, \quad (3)$$

where  $\stackrel{\diamond}{=}$  represented an operator of extended assign as defined.

ii) Next the Recursion ( $l = 1, \dots, L_t$ ) is performed. The weight tensors are of  $W^{(l)}, i, k, c, s$  are expressed below

$$W_{k,c,s}^{(l),i} \stackrel{\diamond}{=} e^{-2\pi i \xi_0^i \cdot (t_s^c - t_k)} \mathcal{L}_k(t_s^c) \quad (4)$$

where  $\xi_0$  represents the centre of  $A^i$ ,  $t_s^c$  represent the Chebyshev points in  $C_c$ .

iii) After the recursion, the Switch ( $l = L_t$ ) is performed, which is a special layer of local operations. Thus an input tensor as  $\lambda^{(L_t)}(i, j, s)$  is expressed in the following equation (5)

$$\lambda^{(L_t)}(i, j, k) = \sum_{s=1}^r W_{k,s}^{(L_t),i,j} \lambda^{(L_t)}(i, j, s) \quad (5)$$

Where the  $W^{(L_t)}, i, j, k, s$  denotes dense weights. Also, the dense weight tensors are represented in equation (6)

$$W_{k,s}^{(L_t),i,j} \stackrel{\diamond}{=} e^{-2\pi i \xi_k^{A_i^{L_t}} \cdot t_s^{B_j^{L_\xi}}} \quad (6)$$

where  $\xi_k^{A_i^{L_t}}$  represents the Chebyshev points in  $A_i^{L_t}$  and  $t_s^{B_j^{L_\xi}}$  are Chebyshev points in  $B_j^{L_\xi}$

iv) Recursion ( $L_t + 1, \dots, L_t + L_\xi$ ). It is performed by a non-mixing channel j where the 1D convolution layer is expressed as,

$$\lambda^{(l)}(i, j, k) = \sum_{s=1}^r \sum_{c=0,1} W_{k,c,s}^{(l),j,a} \lambda^{(l-1)}(\lfloor i/2 \rfloor, 2j+c, s) \quad (7)$$

where  $a = i \bmod 2$ .

v) Interpolation ( $l = L$ ). The weight tensor is represented as  $W^{(L)}, p, 0, k$  is expressed in below equation (8)

$$W_{p,0,k}^{(L)} \stackrel{\diamond}{=} e^{-2\pi i (\xi_p - \xi_k) \cdot t_0} \mathcal{L}_k(\xi_p), \quad 1 \leq p \leq m \text{ and } 1 \leq k \leq r. \quad (8)$$

where  $p = 1, \dots, m$  and  $k = 1, \dots, r$ . based on these processes, the features are extracted in the segmentation process. Then the exact output prediction is identified in the dental care images than the existing ones.

#### 4. Result and Discussion

The result and discussion are presented in this section. This work is simulated and verified using MATLAB software. The results are figured out in the following.

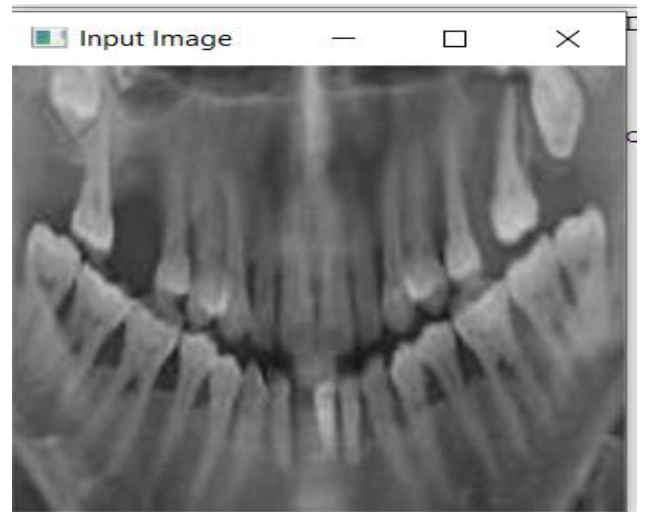


Fig. 3 Input image

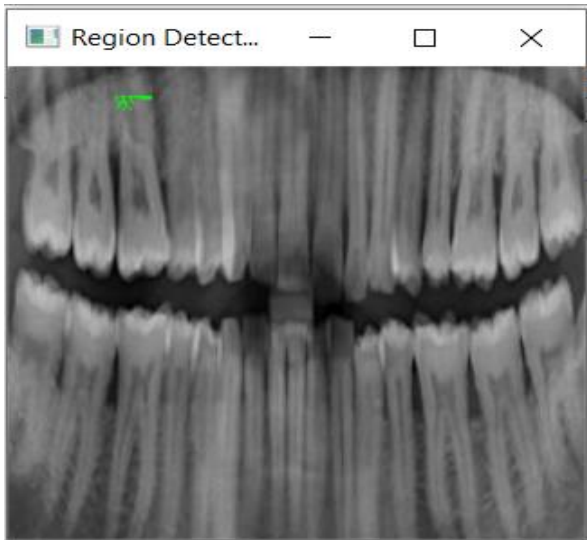


Fig. 4 Output Predicted image

```
-----Stacked Dense RNN-----
[[114  5]
 [  8 129]]
      precision    recall  f1-score   support

         0.0         0.93         0.96         0.95         119
         1.0         0.96         0.94         0.95         137

 accuracy          0.95          0.95          0.95          256
 macro avg          0.95          0.95          0.95          256
 weighted avg          0.95          0.95          0.95          256

TP 115
TN 130
FP 6
FN 9
Sensitivity 92.74193548387096
Specificity 95.58823529411765
Precision 95.0413223140496
Recall 92.74193548387096
NPV 0.935251798561151
FPR 0.04411764705882353
FNR 0.07258064516129033
FDR 0.049586776859504134
Accuracy 94.23076923076923
Support 245
Kappa Coefficient 0.8842455182239106
AUC 94.1650853889943
Error Rate 0.06474820143884892
Jaccard Coefficient 0.8846153846153846
Equal Error Rate -93.1650853889943
False Acceptance Rate 4.411764705882348
False Rejection Rate 7.258064516129039
F-Measure 0.9387755102040817
>>> |
```

References

- [1] Wil G.M.Geraets, and Paul F.Van der Stelt, "Analysis of the Radiographic Trabecular Pattern," *Pattern Recognition Letters*, vol. 12, no. 9, pp. 575-581, 1991. *Crossref*, [https://doi.org/10.1016/0167-8655\(91\)90168-L](https://doi.org/10.1016/0167-8655(91)90168-L)
- [2] Elizabeth B. Claus et al., "Dental X-Rays and Risk of Meningioma," *Cancer*, vol. 118, no. 18, pp. 4530-4537, 2012. *Crossref*, <https://doi.org/10.1002/cncr.26625>
- [3] W T Longstreth Jr et al., "Dental X-Rays and the Risk of Intracranial Meningioma: A Population-Based Case-Control Study," *Cancer*, vol. 100, no. 5, pp. 1026-1034, 2004. *Crossref*, <https://doi.org/10.1002/cncr.20036>
- [4] Wil G. M. Geraets et al., "A New Method for Automatic Recognition of the Radiographic Trabecular Pattern," *Journal of Bone Mineral and Research*, vol. 5, no. 3, pp. 227-233, 1990. *Crossref*, <https://doi.org/10.1002/jbmr.5650050305>
- [5] Wil G. M. Geraets et al., "Detecting Bone Loss Along with Dental Implants by Subtraction of Panoramic Radiographs," *Clinical Oral Implants Research*, vol. 23, no. 7, pp. 861-865, 2012. *Crossref*, <https://doi.org/10.1111/j.1600-0501.2011.02215.x>
- [6] "A Grand Challenge for Automated Detection of Anatomical Landmarks and Analysis for Diagnosis in Cephalometric X-ray Image," 2015. [Online]. Available: <http://www.ntust.edu.tw/~cweiwang/ISBI2015>
- [7] Abdolvahab Ehsani Rad et al., "Digital Dental X-Ray Database for Caries Screening," *3D Research*, vol. 7, 2016. *Crossref*, <https://doi.org/10.1007/s13319-016-0096-5>
- [8] Mahmoud Al-Ayyoub, Ismail Heidi, and Haya Rababah, "Detecting Hand Bone Fractures in X-Ray Images," *Journal of Multimedia Processing and Technologies*, vol. 4, no. 3, pp. 155-168, 2013.

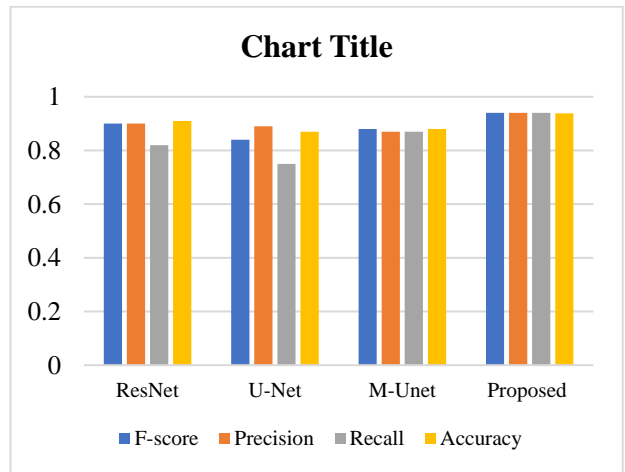


Fig. 5 Performance analysis

Table 1. Comparison Table

	ResNet	U-Net	M-Net	Proposed
<b>F-score</b>	<b>0.9</b>	<b>0.84</b>	<b>0.88</b>	<b>0.94</b>
<b>Precision</b>	<b>0.9</b>	<b>0.89</b>	<b>0.87</b>	<b>0.94</b>
<b>Recall</b>	<b>0.82</b>	<b>0.75</b>	<b>0.87</b>	<b>0.94</b>
<b>Accuracy</b>	<b>0.91</b>	<b>0.87</b>	<b>0.88</b>	<b>0.9383</b>

5. Conclusion

The DL-based butterfly-net technique is presented to segment the dental cavity utilising x-ray input images. This strategy has been executed using conventional image processing techniques by performing segmentation after image enhancement and outlining contour for teeth to complete the segmentation step. Besides, a few features of dental x-ray images are portioned utilising Butterfly Net. The extracted information can be performed to get the teeth estimations for dental determination frameworks. This technique is focused on the feasible classification or determination of dental caries from dental x-ray images. The acquired outcomes exhibit a fulfilled accuracy of cavity detection in the technique.

- [9] Weng-Kong Tam, and Hsi-Jian Lee, "Improving Tooth Outline Detection by Active Appearance Model with Intensity-Diversification in Intraoral Radiographs," *Journal of Information Science and Engineering*, vol. 32, pp. 643-659, 2016.
- [10] Sudhakar T et al., "Automatic Detection and Classification of Brain Tumor using Image Processing Techniques," *Research Journal of Pharmacy and Technology*, vol. 10, no. 11, pp. 3692-3696, 2017. *Crossref*, <https://doi.org/10.5958/0974-360X.2017.00669.2>
- [11] Abdolvahab Ehsani Rad et al., "Evaluation of Current Dental Radiographs Segmentation Approaches in Computer-Aided Applications," *IETE Technical Review*, vol. 30, no. 3, pp. 210-222, 2013. *Crossref*, <https://doi.org/10.4103/0256-4602.113498>
- [12] R BalaSubramanyam et al., "Different Image Segmentation Techniques for Dental Image Extraction," *International Journal of Engineering Research and Applications*, vol. 4, no. 7, pp. 173-177, 2014.
- [13] Y. H. Lai, and P. L. Lin, "Effective Segmentation for Dental X-Ray Images Using Texture Based Fuzzy Inference System," *ACIVS LNCS Springer Verlag Berlin Heidelberg*, pp. 936-948, 2008. *Crossref*, [https://doi.org/10.1007/978-3-540-88458-3\\_85](https://doi.org/10.1007/978-3-540-88458-3_85)
- [14] Abdolvahab Ehsani Rad et al., "Digital Dental X-Ray Image Segmentation and Feature Extraction," *Telkomnika*, vol. 11, no. 6, pp. 3109-3114, 2013. *Crossref*, <https://doi.org/10.11591/telkomnika.v11i6.2655>
- [15] Bethanney Janney J, and S. Emalda Roslin, "Classification of Melanoma from Dermoscopic Data Using Machine Learning Techniques," *Multimedia Tools and Applications*, vol. 79, pp. 3713-3728, 2020. *Crossref*, <https://doi.org/10.1007/s11042-018-6927-z>
- [16] Sukumar Ponnusamy, and Ramasamy Kannan Gnanamurthy, "Computer-Aided Detection of Cervical Cancer Using Pap Smear Images Based on Adaptive Neuro-Fuzzy Inference System Classifier," *Journal of Medical Imaging and Health Informatics*, vol. 6, no. 2, pp. 312-319, 2016. *Crossref*, <https://doi.org/10.1166/jmih.2016.1690>